ELSEVIER

Journal of Alloys and Compounds 444–445 (2007) 191–196

Journal of ALLOYS AND COMPOUNDS

www.elsevier.com/locate/jallcom

# Thermodynamic, alloying and defect properties of plutonium: Density-functional calculations

G. Robert [a,*], A. Pasturel [b], B. Siberchicot [a]

[a] *CEA-DIF, BP 12, F-91680 Bruyéres-le-Châtel, France*

[b] *Laboratoire de Physique et Moderation des Milieux Condensés, CNRS, 25 Avenue des Martyrs, BP 106, F-39042 Grenoble, France*

Received 27 June 2006; received in revised form 18 September 2006; accepted 21 September 2006
Available online 2 November 2006

**Abstract**

We show that thermodynamic properties of Pu metal as well as those of $Pu_{(1-x)}M_x$ (M = Al, Ga, In) compounds are poorly described by traditional DFT but rather well modeled when including magnetic interactions. The cluster variation method is used to emphasize that the presence of Ga atoms in the δ-Pu phase leads to an important chemical short-range order which stabilizes this phase as a function of temperature and composition. Our results indicate also that Ga atoms introduce local strain fields in δ phase which relax with increasing distance from the Ga atoms. Finally we show that local relaxations are also essential to predict correct vacancy formation and migration energies in this phase.


*Keywords:* Metals; Crystal structure and symmetry; EXAFS; Point defects; Crystal binding and equation of state

## 1. Introduction

Since Seaborg, Mc Millan, Kennedy and Wahl isolated plutonium in 1941 and despite 65 years of research, a fine understanding of this metal and its alloying effects remains a challenge. It is mainly due to the fact that 5f electrons sit at the boundary between localization and itinerancy. From this ambiguity results a strong sensibility at the least perturbation. If at low temperature, plutonium exhibits very open complex structures (α and β monoclinic), more compact structures appear (γ tetragonal; δ, δ′, ε cubic) before melting at 913 K. Under low pressure (few kbar), three of them disappear (γ, δ, and δ′) [1]. These structural changes are accompanied by dramatic changes in physical properties like density (more than 25% between α and δ phase), thermal expansion (negative for δ and δ′, very large for the others) or elastic and mechanical properties [2]. Unlike the brittle α monoclinic structure, stable at ambient conditions, the high temperature cubic δ phase is ductile. Then, an extension of its range of (meta) stability is necessary for engineering application. This can be done by small additions of alloying elements like IIIB metal (Al, Ga or under quenching In). Compared to δ-Pu phase, this small perturbation brings significant changes in some properties: the thermal expansion coefficient becomes positive [3] and local relaxations seem to depend on impurity concentrations [4,5].

Aging effects in this complex material can also alter phase stability or mechanical properties. The decay of plutonium atoms into an uranium nucleus and a helium nucleus produces displacement damages. Helium can be trapped in vacancies, then accumulate and form helium bubbles. This local distortion can create local pressure or swelling. The knowledge of activation energy of these processes (migration plus vacancy energies) as well as theirs effects, which drive local relaxations, is inestimable to understand thermodynamic and kinetic behaviors of these alloys [6,7].

*Ab initio* methods are well designed to calculate the specificities of compounds for which it is difficult to carry out experimental measurements and as a starting point in multi-scale studies. Unfortunately, if density-functional treatments (DFT) in the local density approximation (LDA) are able to reproduce roughly the main properties of the α phase, such approaches fail to describe any properties of the δ phase. To remedy this, one of the most promising techniques is the dynamical mean field theory (DMFT) [8,9]. But, if such calculations can give us a fine description and some keys in order to obtain a better understanding on the role played by electronic structure (dynamical

* Corresponding author. Tel.: +33 169266506.
*E-mail address:* gregory.robert@cea.fr (G. Robert).

0925-8388/$ – see front matter © 2006 Elsevier B.V. All rights reserved.
doi:10.1016/j.jallcom.2006.09.118

fluctuation), two main drawbacks limit this approach: computer time retrains DMFT to small system (1–4 atoms) and the results are $U$-dependent (where $U$ is the Hubbard parameter which governs the Coulomb repulsion energy). In a material with so many phases, $U$ parameter can vary in function of phases (from 4 eV in δ phase to almost 0 in α phase), pressure or alloying amount, and predictive calculations can hardly be done.

On the other hand, using generalized gradient approximation (GGA) and spin polarization (SP) calculations bring strong improvements on numerous properties of all allotropes of plutonium and its alloys: equilibrium volumes, bulk moduli, elastic properties or energy differences [9].

However, if ordered compound $PuGa_2$ or $PuGa_3$ show a strong anti-ferromagnetic coupling or if simply dissolving hydrogen in plutonium is enough to make the system ferromagnetic, there is no experimental evidence of magnetic moments in plutonium or weakly alloyed plutonium with gallium [10]. Nevertheless, the amount of coherent results points out that calculations within spin polarization (SP) GGA framework can reproduce at least qualitatively macroscopic properties. Moreover, numerical efficiency of such method allows us to predict or estimate properties for large systems [11].

In this paper, we apply GGA-SP to various properties of plutonium and its alloys in order to understand the stabilization phenomena and to obtain physical values as input for other theoretical tools (classical potential or Monte-Carlo method) within the limits and the accuracy of this approach. The electronic calculations are based on two methods that have distinct qualities. The most accurate method, which is also the most CPU expensive, is an all-electron LAPW method [12]. The second is based on projected augmented wave (PAW) pseudo-potential approach [13] with a plane-wave basis set that enables efficient calculations of forces and relaxations on large systems.

More details on these computational techniques can be found in our previous papers [14–18]. The remainder of the paper is organized as follows: in Section 2, we present a review of some previous calculations on plutonium and its neighbors [14,15]; in Section 3, we extend this review to ordered compounds of plutonium and on stability in δ-Pu alloys [16,17]; Section 4 describes work in progress on local relaxations in the δ-Pu–Ga solid solution while Section 5 presents a study on the self-diffusion of vacancies in δ-Pu [18].

## 2. Structural stabilities and equation of state (EOS) for plutonium and its neighbors

It seems clear from literature and from our calculations [14] that non-spin-polarized (NSP) DFT (cross in Fig. 1) fails to reproduce equilibrium volumes (square in Figs. 1 and 2) as well as elastic properties or cohesive energies of compact structures of plutonium (5.18 eV for δ phase). It is also true for heavy actinides (Am to Lw). Experimentally and from thermodynamic considerations, the most stable cubic structure at zero temperature should be a body centered cubic (bcc) for Np and face-centered structure (fcc) for Am and Cm. Using GGA-NSP, bcc-Np or α-Pu phases are energetically favored but bcc structures are predicted lower in energy than fcc for heavy actinides.

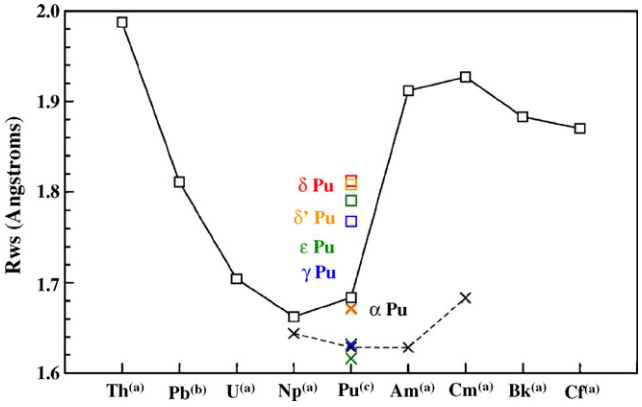


Fig. 1. Calculated equilibrium volume without spin polarization are reproduced by cross (color online). Experimental equilibrium volume (squares) for plutonium allotropes and its neighbors: (a), (b) and (c) are for Refs. [27–29], respectively.

Taking into account spin polarization leads to strong changes in the EOS of compact structures of plutonium but also on americium and curium (star in Fig. 2). These transformations in properties of the ground state are accompanied by large changes in structural stabilities but also on energy differences. If taking into account spin polarization in calculations weakly affects equilibrium properties (i.e. equilibrium volume, elastic properties or total energies) of Np or α-Pu, this approach strongly modifies results for Am, Cm or other allotropes of plutonium. For americium or curium, the total energy is lowered by 1.3 and 1.9 eV/atom, respectively. For δ and δ′ phases of Pu, total energy is reduced approximately by 0.5, 0.3 eV/atom for γ phase and 0.2 eV/atom for $\varepsilon$. As the total energy of α-Pu is almost unchanged (less than 0.05 eV/atom), GGA-SP allows us to reproduce the right energy sequence with energy differences close to experimental data. These results are in agreement with the works of Skriver et al. or Antropov et al. and more recent values obtained by Kutepov and Kutepova [9] on α and δ plutonium or those obtained by Niklasson et al. [19] from thorium to californium using a model based on disordered local moments

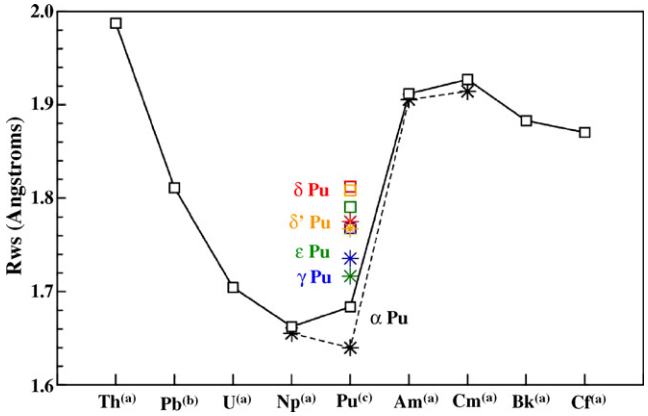


Fig. 2. Calculated equilibrium volume (star) with anti-ferromagnetic order (color online). Experimental equilibrium volume (squares) for plutonium allotropes and its neighbors: (a), (b) and (c) are for Refs. [27–29], respectively.

(DLM). Söderlind et al. [9,20] investigated several magnetic configurations including DLM with the same success on these properties. These results seem to confirm that the apparition of large spin moment in GGA can be viewed as an indication of strong electron correlations. Taking into account spin–orbit coupling (SOC) mainly affects equilibrium volume but in lesser manner than SP (some few percent) and leaves nearly unchanged energy differences between phases or elastic properties [21].

Other properties are also improved. For example, equilibrium volumes of compact phases of plutonium or heavy actinides are reproduced within 5–10%. It is a strong improvement compared to the 30% inaccuracy (a factor of 2 for Am and Cm) for γ, δ, δ′ and ε-Pu without SP. Cohesive energy of the δ-Pu phase is also reduced to a more reasonable value of 3.8 eV. At experimental volume the δ phase is found mechanically stable and the values of elastic constants are roughly reproduced.

The general agreement between experimental trends and the structural hierarchy obtained at $T = 0$ K incited us to study the thermodynamic properties of Pu as a function of temperature and pressure using a simple Debye–Gruneisen model [15]. It is noteworthy that if this model suffers of some crude approximations which will make impossible to reproduce all experimental specificities of plutonium like negative thermal expansion for the δ phase, such an approach can only allow us to estimate the different thermal contributions. Within this framework, we first calculate Gibbs energies as function of pressure for different structures.

Then it is possible to obtain the solid part of the Pu phase diagram including α, γ, δ and ε phases (Fig. 3). We can evaluate to at least 60% the part of Helmholtz free energy due to the ionic thermal term. But the quasi-harmonic approximation is not sufficient to obtain a correct description of thermal properties of different allotropes. More particularly, the electronic contribution for the γ, δ and ε as well as the anharmonic contribution for the ε phase play an important role to determine the transition temperatures. Nevertheless, we emphasize that accurately evaluating each of these contributions remains a challenge for the actual DFT-based calculations.

## 3. Structural stability of $Pu_{(1-x)}M_x$ (M = Al, Ga and In) compounds and phase stability of δ-Pu alloys

Concerning Pu-based alloys, few total energy calculations have appeared since the pioneering band structure study of Weinberger et al. [22]. Formation energies are extracted from the total energies by subtracting the concentration weighted total energies of pure fcc Pu and X (X = Al, Ga or In) from the fcc structure. The calculated formation energies of $Pu_3M$ are in disagreement with experiment since these calculations use only the local density approximation to treat electron-exchange and correlation effects [22]. Very recently, the stability of some Pu-based alloys has been studied using the standard spin-polarized GGA approach. Calculations based either on the KKR method within the atomic sphere approximation [23] or ours on the LAPW or PAW method [17] lead to calculated lattice constants of $Pu_3M$ compounds in excellent agreement with experiment. Also, these compounds display strong negative values of formation energies, which characterize Pu–M systems as presenting strong attractive interactions (Fig. 4) in agreement with the experimentally known behavior [24]. Let us mention in our calculations that for each volume, the structure is optimised with respect to all degrees of freedom allowed by its space-group symmetry.

It has been argued that alloying effects do not depend on long-range magnetic ordering [16]. To give a proof based on energetic arguments, we compared the cohesive energies of the $L1_0$ structure of PuGa with five different magnetic configurations. The differences between all these configurations are small (less than 13 meV/atom) with respect to the formation energies of the $L1_0$ compound (480 meV/atom) and indicate that the long-range magnetic ordering does not contribute to the alloying effects between Pu and Ga. The effect of spin–orbit coupling is similar to that obtained for plutonium i.e. it affects mainly the equilibrium volume but in lesser manner than SP (some few percent) and it leaves energy differences nearly unchanged.

More interesting, these strong attractive interactions favor the occurrence of fcc superstructures in Pu–In while more complex structures are energetically the most stable ones in the two other

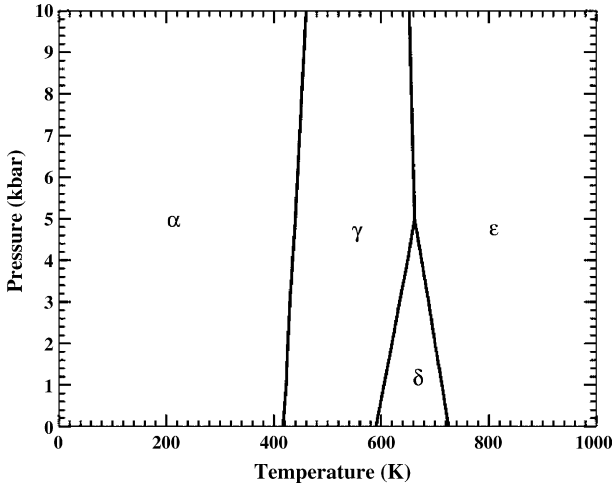


Fig. 3. The calculated phase diagram [15].

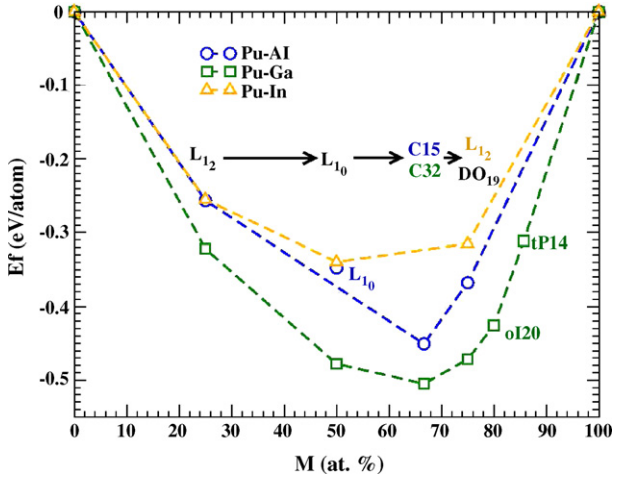


Fig. 4. Formation energies of Pu–M alloys for several structures using the GGA-SP (color online).

systems (Fig. 4). In the Pu–Ga system, $PuGa_2$ in the C32 structure and $PuGa_3$ in the $D0_{19}$ structure are found to be the most stable phases in the Ga-rich side. In the Pu–Al system, $PuAl_2$ in the C15 structure and the prototype hexagonal $D0_{19}$ structure are the most stable in the Al-rich side. Therefore, we can conclude that GGA spin-polarized calculations are able to reproduce the high negative values of formation energies as well as the different structural hierarchies observed in the three systems.

In order to gain insight at the microscopic level into the phase stability of $Pu_{(1-x)}M_x$ compounds, we inspect the partial densities of states (DOS) in function of the δ-stabilizer amount [16]. As a consequence of local atomic environment, the structural stability is governed by the competition between Pu(5f)–Pu(6d), M(p)–Pu(6d) and M(s,p)–M(s,p) interactions. Another striking feature is the presence of a gap related to sp bands in the bottom area of the DOS and its concentration-dependent location and width. It may be emphasized that the main effect of spin polarization is to push the occupied 5f and 6d states to lower energies. Thus, hybridization with the wide M(sp) band occurs at lower energies, which explains the more negative formation energies.

From these results, we can perform an accurate Ising-like cluster expansion and study the stability of the δ phase as a function of temperature and composition. Such a model is parameterized by a set of effective cluster interactions (ECIs), which are dependent on the local atomic configurations.

From these ECIs obtained from fcc superstructures, we are able to obtain the Gibbs energy of mixing of the δ solid solution [17]. The most important result is that taking into account the chemical short-range order (CSRO) within the framework of the cluster variation method (CVM) leads to a strong stabilization of δ Pu–M solid solutions (Fig. 5 reproduces results obtained on Pu–Ga system). Once again, DFT calculations based on GGA-SP are able to reproduce many properties of Pu–M alloys. The CVM treatment underlines the essential role played by the CSRO in the stabilization of plutonium-based solid solutions.

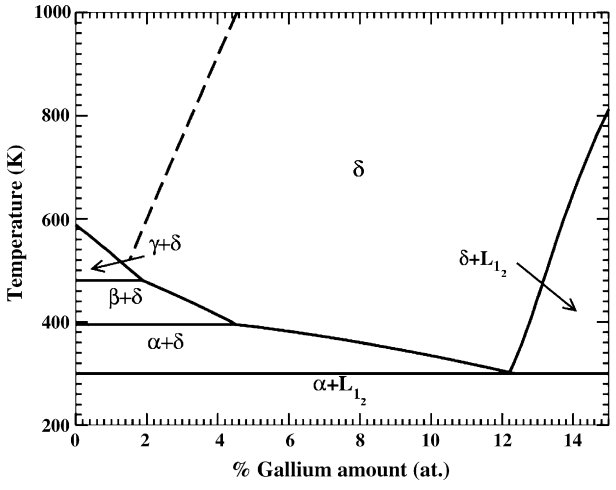


Fig. 5. Calculated solid Pu-rich part of the Pu–Ga phase diagram. Dashed line: solubility limit of Ga in δ-Pu without CSRO (ideal entropy of mixing). Full line: complete phase diagram with CSRO.

## 4. Local relaxation around gallium impurity

EXAFS data [5] show significant departure from fcc behavior for the Pu atoms neighboring a Ga atom in a 3.3 at.% Ga δ-stabilized Pu. Faure et al. [4] have studied such a behavior as function of Ga composition. While non-spin-polarized LDA calculations do not reproduce the experimental interatomic distance [25], in a very recent study, Sadigh and Wolfer [11] have shown that spin-polarized DFT is able to predict the observed departure from fcc symmetry for an alloy composition of 3.2 at.% Ga. Here, we propose to study plutonium–plutonium and plutonium–gallium distances as a function of composition using a supercell of 108 atoms. Five different compositions have been chosen up to 10 at.% Ga.

For the two last ones, namely 6.5 and 9.2 at.% Ga, three different configurations have been used, each of them displaying CSRO similar to that obtained by the CVM treatment. In Tables 1 and 2, we report Pu–Pu and Pu–Ga averaged interatomic distances of the first three shells divided by distances obtained in the case of a perfect fcc lattice. A preliminary analysis indicates that plutonium–gallium interatomic distances are shorter than plutonium–plutonium interatomic distances in the first shell while it is the opposite case in the second shell for all the studied compositions. In the third shell, interatomic distances are quite similar, showing that relaxation effects display a short-range character. The standard deviation $\sigma$ points out that local environments around both Pu and Ga atoms are disordered. For instance, for 3.7 at.% Ga, a difference of ≈0.1 Å (≈0.3 Å) is obtained between the shortest and the longest bonds around gallium (plutonium) atom in the first shell. These values indicate that the local structure around Pu atoms is more disordered than the structure around Ga atoms. Such a behavior is in close agreement with results obtained by Cox et al. [5]. Let us mention that this local disorder increases with composition (almost 0.5 Å).

Table 1
Pu–Pu interatomic distances for successive shell divided by distance obtained for these shells in a perfect fcc lattice, $\sigma$ is the standard deviation

| Ga (at.%) | First shell | $\sigma$ | Second shell | $\sigma$ | Third shell | $\sigma$ |
|---|---|---|---|---|---|---|
| 0.9 | 1.001 | 0.048 | 1.000 | 0.071 | 1.000 | 0.062 |
| 1.9 | 1.002 | 0.065 | 0.999 | 0.085 | 1.000 | 0.079 |
| 3.7 | 1.003 | 0.083 | 0.998 | 0.119 | 1.000 | 0.107 |
| 6.5 | 1.005 | 0.127 | 0.996 | 0.184 | 1.000 | 0.157 |
| 9.3 | 1.006 | 0.138 | 0.995 | 0.198 | 1.000 | 0.169 |

Table 2
Pu–Ga interatomic distances for successive shell divided by distance obtained for these shells in a perfect fcc lattice, $\sigma$ is the standard deviation

| Ga (at.%) | First shell | $\sigma$ | Second shell | $\sigma$ | Third shell | $\sigma$ |
|---|---|---|---|---|---|---|
| 0.9 | 0.950 | 0.000 | 1.018 | 0.000 | 0.990 | 0.000 |
| 1.9 | 0.956 | 0.001 | 1.023 | 0.012 | 0.995 | 0.022 |
| 3.7 | 0.958 | 0.044 | 1.021 | 0.033 | 0.995 | 0.036 |
| 6.5 | 0.967 | 0.062 | 1.030 | 0.140 | 1.001 | 0.102 |
| 9.3 | 0.973 | 0.080 | 1.025 | 0.103 | 1.001 | 0.110 |

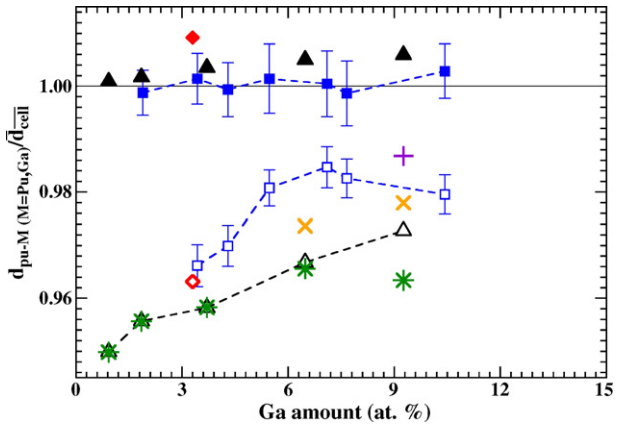


Fig. 6. Interatomic distances divided by first shell distance in a perfect fcc lattice as function of Ga composition. Full symbols (■, ◆, ■): Pu–Pu ratio. Empty symbol (□, ◇, △): Pu–Ga ratio. Squares (■, □) reproduced experimental values obtained by Faure et al. [4] and diamond (◆, ◇) those obtained by Cox et al. [5]. Theoretical ratio are symbolized by triangle (▲, △). Star (✳), cross (✕) and plus (+) represents Pu–Ga distances with 1, 2 and 3 nearest neighbor Ga atoms, respectively (color online).

Fig. 6 shows interatomic distances divided by the distance of the first shell of a perfect fcc lattice as function of Ga composition. The agreement between our calculations and experimental results is good. Moreover, we find that the Pu–Ga distance depends on the number of Ga atoms in the first nearest neighbor (nn) shell of Pu atoms. For instance, Pu–Ga distances are higher for Pu atoms with three Ga atoms (+ in Fig. 6) in their first shell (as observed in 9.8 at.% Ga alloy) than for Pu atoms with two Ga atoms (✕ in Fig. 6). These latter ones are also higher than Pu–Ga distances obtained for Pu atoms with only one nearest neighbor Ga atom (✳ in Fig. 6). These results seem quite independent of Ga composition. Moreover, we can observe that Pu–Ga distances for Pu atoms with three nearest neighbor Ga atoms are similar to those found in the $Pu_3Ga$ compound (in the $L1_2$ structure). Then we can conclude that the evolution of the averaged Pu–Ga distance as a function of Ga composition is related to the increasing number of Pu atoms with three or more Ga atoms in their nearest neighbor shells. It is important to emphasize that the percentage of such Pu clusters increases with Ga composition but depends also on CSRO of δ-Pu–Ga solid solution and then on its thermal treatment.

## 5. Vacancy and migration energy in delta plutonium

As a first step, we study the influence of magnetic configurations on mono- and di-vacancies energies, namely antiferromagnetic (AFM), ferromagnetic (FM) and disordered magnetic structures (DM).

For unrelaxed ionic positions, both mono- and di-vacancies are not very sensitive to the long-range magnetic ordering. It is due to the fact that the bonding properties of δ-Pu originate mainly in the formation of a local spin moment in Pu atoms which strongly modifies the hybridization of the 5f states with other s, p, and d states with respect to non-magnetic calculations [21].

The vacancy formation energy represents around 40% of the Pu cohesive energy (around 1.5 eV) as usually found for transition metals. It is a great improvement compared to the value of 0.5 eV obtained without spin polarization [26]. The other important point is that the formation of di-vacancies does not require additional energy with respect to the formation of two isolated mono-vacancies. This result indicates that vacancy clusters are as stable as isolated vacancies. Such vacancy clusters eventually lead to the nucleation and subsequent growth of voids. However, it is clear that such a process is thermally activated via the diffusion of mono-vacancies to form clusters.

If atomic relaxations are taken into account, the inward relaxation is of the order of 3% (7% for di-vacancies), as usual for transition metals. The energy of the di-vacancy is still similar to the energy of two isolated vacancies. Nevertheless, the relaxed energy and the forces acting on atoms are more sensitive to the magnetic configuration: the relaxed energy is more important for the disordered (DM) (≈0.5 eV) than for the ordered (FM-AFM) (≈0.2 eV) magnetic configuration. For DM, the absence of the long-range magnetic ordering can create a more complex variation of the local spin moment in Pu atoms according to their locations with respect to the vacancy. Without spin polarization, relaxation effects lead to an exothermic value of the vacancy formation energy (−3.5 eV) [26]. Once again, these results underline the importance of spin polarization in such calculations.

In a work in progress, we expand this approach in order to obtain a reliable value on the migration energy of a vacancy. Preliminary results have been obtained for FM ordered cells with 108 atoms. The climbing image nudged elastic band (NEB) [30] method has been applied to determine the potential energy barrier. Typically three slab replicas between the initial and final states are sufficient to produce a smooth minimum energy path. Such calculations give us an encouraging value of 0.85 eV.

We can expect that DFT–GGA-SP-based calculations are also able to give us reasonable values or keys in order to understand defect properties in these alive materials.

## 6. Conclusion

In this paper, we have presented a review of our spin-polarized DFT calculations for thermodynamic and point defects of Pu as well as for thermodynamic and structural properties of δ phase Pu–Ga alloys. Based on these calculations, we conclude that SP-DFT are able to give energy differences between the different allotropes which are consistent with the gross features of the experimental phase diagram of Pu. The CVM treatment of CSRO leads to a strong stabilization of the δ-Pu–Ga solid solution as a function of composition and temperature. The effects on local deformations on the stability of the solid solution have been studied by using supercell techniques including CSRO. We find that spin-polarized DFT accurately predicts Pu–Ga bond lengths as compared to recent EXAFS measurements. For the vacancy-formation in δ-Pu, we find that the formation energy is higher than the migration energy, which is in agreement with the experimental results.

## References


[1] D.A. Young, Phase Diagrams of the Elements, University of California Press, Oxford, England, 1991.
[2] S.S. Hecker, D.R. Harbur, T.G. Zocco, Prog. Mater. Sci. 49 (2004) 429.
[3] J.A. Lee, G.T. Meaden, R.O.A. Hall, E. King, in: E. Grison, W.B.H. Lord, R.D. Fowler (Eds.), Plutonium 1960, Cleaver-Hume Press Ltd., London, 1961.
[4] P. Faure, B. Deslandes, D. Bazin, C. Tailland, R. Doukhan, J.M. Fournier, A. Falanga, J. Alloy Compd. 244 (1996) 131.
[5] L.E. Cox, R. Martinez, J.H. Nickel, S.D. Conradson, P.G. Allen, Phys. Rev. B 51 (1995) 751.
[6] S.S. Hecker, Challenges in Plutonium Science, Los Alamos Science 26 (2000) 290.
[7] M.J. Fluss, B.D. Wirth, M. Wall, T.E. Felter, M.J. Caturla, A. Kubota, T.D. de la Rubia, J. Alloy Compd. 368 (2004) 62.
[8] S.Y. Savrasov, G. Kotliar, E. Abrahams, Nature (London) 410 (2001) 793; X. Dai, S.Y. Savrasov, G. Kotliar, A. Migliori, H. Ledbetter, E. Abrahams, Science 300 (2003) 953.
[9] H.L. Skriver, O.K. Andersen, B. Johansson, Phys. Rev. Lett. 41 (1978) 42; H.L. Skriver, O.K. Andersen, B. Johansson, Phys. Rev. Lett. 44 (1980) 1230;
V.P. Antropov, M. Van Schilfgaarde, B.N. Harmon, J. Magn, Magn. Mater. 140–144 (1995) 1355;
Y. Wang, Y.F. Sun, J. Phys. Condens. Mat. 12 (2000) L311;
P. Söderlind, A. Landa, B. Sadigh, Phys. Rev. B 66 (2002) 205109;
A.I. Kutepov, S.G. Kutepova, J. Phys. Condens. Mat. 15 (2003) 2607.
[10] P. Boulet, E. Colineau, P. Javorsky, F. Wastin, J. Rebizant, J. Alloy Compd. 394 (2005) 93;
R.H. Heffner, et al., Physica B 374/375 (2006) 163;
R.H. Heffner, et al., Phys. Rev. B 73 (2006) 094453;
N.J. Curro, L. Morales, Mater. Res. Soc. Symp. Proc. 802 (2004) 53.
[11] B. Sadigh, W.G. Wolfer, Phys. Rev. B 72 (2005) 205122.
[12] P. Blaha, K. Schwarz, G. Madsen, D. Kvasnicka, J. Luitz, WIEN2k, Tech. Universität Wien, Austria, 2001.
[13] G. Kresse, D. Joubert, Phys. Rev. B 59 (1999) 1758.
[14] G. Robert, Etude du plutonium et de ses alliages avec les éléments de la colonne IIIB, PhD Thesis, Université Paris VI, 2003.
[15] G. Robert, A. Pasturel, B. Siberchicot, J. Phys. Condens. Mat. 15 (2003) 8377.
[16] G. Robert, A. Pasturel, B. Siberchicot, Phys. Rev. B 68 (2003) 075109.
[17] G. Robert, C. Colinet, B. Siberchicot, A. Pasturel, Philos. Mag. 84 (2004) 1877;
G. Robert, C. Colinet, B. Siberchicot, A. Pasturel, Model. Simul. Mater. Sci. Eng. 12 (2004) 693.
[18] G. Robert, A. Pasturel, B. Siberchicot, Europhys. Lett. 71 (2005) 412.
[19] A.M.N. Niklasson, J.M. Wills, M.I. Katsnelson, I.A. Abrikosov, O. Eriksson, B. Johansson, Phys. Rev. B 67 (2003) 235105.
[20] P. Söderlind, Europhys. Lett. 55 (2001) 525.
[21] P. Söderlind, B. Sadigh, Phys. Rev. Lett. 92 (2004) 185702.
[22] P. Weinberger, A.M. Boring, J.L. Smith, Phys. Rev. B 31 (1985) 1964; P. Weinberger, A. Gonis, A.J. Freeman, A.M. Boring, Phys. Rev. B 31 (1985) 1971.
[23] A. Landa, P. Söderlind, J. Alloy Compd. 354 (2003) 99.
[24] C. Colinet, A. Pasturel, in: K.A. Gschneidner Jr., L.R. Eyring (Eds.), Handbook on the Physics, Chemistry of Rare Earths, vol. 19: Lanthanides/Actinides Physics-II, North Holland, 1994.
[25] J.D. Becker, B.R. Cooper, J.M. Wills, L. Cox, Phys. Rev. B 58 (1998) 5143.
[26] G. Jomard, Private communication: PAW calculations on 32 atoms cell and at theoretical equilibrium volume.
[27] C.N. Sigman, J. Chem. Educ. 61 (1984) 137.
[28] J.W. Ward, P.D. Kleinschmidt, D.E. Peterson, in: A.J. Freeman, C. Keller (Eds.), Handbook on the Physics and Chemistry of the Actinides, vol. 4, North-Holland, Amsterdam, 1986 (Chapter 7).
[29] J. Donohue, The Structure of the Elements, John Wiley and Sons Ltd., New York, 1974.
[30] G. Mills, H. Jonsson, G.K. Schenter, Surf. Sci. 324 (1995) 305; H. Jonsson, G. Mills, K.W. Jacobsen, in: B.J. Berne, G. Ciccotti, D.F. Coker (Eds.), Classical and Quantum Dynamics in Condensed Phase Simulations, World Scientific, 1998.